Shape-controlled Synthesis of Activated Bio-chars by Surfactant-templated Ionothermal Carbonization in Acidic Ionic Liquid and Activation with Carbon Dioxide

Feng Guo and Zhen Fang*

Shape-controlled bio-chars were synthesized in two steps: (i) ionothermal carbonization of biomass (*e.g.*, glucose, cellulose, lignin, and bamboo) at low temperatures (150 to 180 °C) in an acidic ionic liquid (IL), and (ii) subsequent activation with carbon dioxide at higher temperature (500 °C). Acidic IL was used as both the medium and catalyst for advanced carbon materials production. During the first step the primary structures of spherical particles were obtained. The surfactants sodium dodecyl sulfonate (SDS), ethylene glycol (EG), and sodium oleate (SO) were also used to modify the surface morphology of bio-chars and activated bio-chars. After the second step, the primary structures of bio-chars were still preserved or improved. The Brunauer-Emmett-Teller surface area and the pore diameter of activated bio-chars were 289 to 469 m^2/g and 3.5 to 3.6 nm, respectively. Scanning electron microscope and transmission electron microscope images show that after modification of bio-chars with SDS, EG, and SO, activated bio-char particles agglomerated into rod-like (~200 nm diameter), nano-membrane (~70 nm thickness), and spherical (~200 nm) morphologies, respectively. The morphology of activated bio-chars was easily controlled during the synthesis, which is important for the exploitation of their peculiar properties and unique applications.

Keywords: Bio-chars; Acidic ionic liquid; Carbonization; Modification; Surfactants; Activation

Contact information: Biomass Group, Key Laboratory of Tropical Plant Resource and Sustainable Use, Xishuangbanna Tropical Botanical Garden, Chinese Academy of Sciences, 88 Xuefu Road, Kunming, Yunnan Province 650223, China;
** Corresponding author: zhenfang@xtbg.ac.cn (ZF), guofeng@xtbg.ac.cn(FG)*

INTRODUCTION

Activated carbons attract much attention and are applied in a wide range of fields because of their high Brunauer-Emmett-Teller (BET) surface area, micro to macropores, and light weight (Gao *et al.* 2013; Hu and Srinivasan 2001; Ioannidou and Zabaniotou 2007; Sircar *et al.* 1996). They have been widely used in catalyst support (Guo *et al.* 2012a, 2012b; Wu *et al.* 2012), energy storage (Simon and Gogotsi 2008; Stoller *et al.* 2008), adsorption (Choma *et al.* 2011; Danish *et al.* 2013; Kruk *et al.* 1996) and adsorptive separation (Deng *et al.* 2013; Sircar *et al.* 1996). Biomass materials, including coconut shells (Hu and Srinivasan 1999; Li *et al.* 2008; Sekar *et al.* 2004), bamboo (Hameed *et al.* 2007; Mizuta *et al.* 2004), and other wood materials (Carrott and Ribeiro Carrott 2007; Danish *et al.* 2013; Ioannidou and Zabaniotou 2007; Titirici and Antonietti 2010) are used for the production of activated carbons. In general, the surface morphology and pore structure of activated carbons determine their emerging applications. Therefore, it is important to design and construct activated carbons with

special architectures. As an alternative to high-temperature pyrolysis (~800 °C), hydrothermal carbonization (>200 °C) has been used to produce highly functionalized carbon materials with specific properties (Liu *et al.* 2013; Sevilla and Fuertes 2009; Titirici and Antonietti 2010). Sevilla and Fuertes (2006) prepared a series hydrochars by hydrothermal carbonization of saccharides at temperatures of 170 to 240 °C, and a high degree of unified spherical morphologic particles (0.4 to 0.6 μm) was obtained. However, this process requires high-pressure conditions and produces mostly micro-spherical particles. Moreover, carbon membranes are difficult to prepare using hydrothermal processes (Lee *et al.* 2010a). Currently, this goal is primarily achieved by a self-assembly process. However, the organic compound resorcinol/formaldehyde has been used as carbon precursor (Wang *et al.* 2008).

Ionic liquids (ILs), defined as salts composed solely of cations and anions that melt at or below about 100 °C, have emerged as potential solvents (Welton 2004). ILs are capable of dissolving biomass quickly and effectively, due to hydrogen-bonding interactions between the cations of the precursor and the anions of the ILs (Guo *et al.* 2012a). ILs may be ideal substitutes of traditional solvents due to their thermal stability, non-volatility, negligible vapor pressure, and high boiling point (Earle and Seddon 2000). They can be regarded as ideal reaction media for biomass carbonization under ambient pressures. Therefore, a novel ionothermal method based on ILs as precursors or solvents for carbonization has been reported (Earle and Seddon 2000; Lee *et al.* 2009, 2010b; Paraknowitsch and Thomas 2012; Wang and Dai 2010; Welton 2004). When ILs are used as reaction media for ionothermal carbonization, the structural morphology of the resultant carbon materials depend upon the primal construction of ILs (Lee *et al.* 2010b). In addition, the high cost of ILs is an obstacle for their large-scale application.

Ionic liquids have long been used as reaction media for materials syntheses but are not often used in the preparation of porous carbon materials (Demir-Cakan *et al.* 2010; Lee *et al.* 2010b; Paraknowitsch and Thomas 2012; Wang and Dai 2010; Yuan *et al.* 2010; Xie *et al.* 2011). Moreover, less work has been reported on the chemical and structural properties of the resultant carbon products. Hence, the objective of this work is to develop a novel two-step process for the production of activated bio-chars from biomass (*e.g.*, glucose, cellulose, lignin, and bamboo) through a modified ionothermal carbonization step in an acidic IL at low temperatures (150 to 180 °C) and an activation step at high temperature (500 °C). Herein, acidic IL was used as both the medium and acid catalyst for carbon materials preparation. Different surfactants were also studied with the aim to improve the surface morphology of bio-chars at the ionothermal carbonization step in an acidic IL. The chemical properties and structural characteristics of bio-chars were analyzed by various techniques.

EXPERIMENTAL

Materials

Anhydrous glucose (purity > 99%) was obtained from Bomei Chem. Co., Ltd. (Hefei, Anhui). Cellulose (powder; about 50 μm particle size) was purchased from J&K Scientific Ltd. (Beijing). Lignin and sodium oleate (SO) were from Tokyo Chem. Co., Ltd. Bamboo powders were supplied by Anji Corp. (Anji, Zhejiang). Ethylene glycol (EG) was from Xilong Chem. Co., Ltd. (99% purity, Shantou, Guangdong) and sodium dodecyl sulfonate (SDS) from Shanghai Chemical Reagent Factory. An IL, 1-sulfobutyl-

3-methylimidazolium hydrogen sulfate {[SBMIM][HSO_4]} (purity > 99%, halide content ≤ 800 ppm) was purchased from Chengjie Chemical Co. (Shanghai) and used for carbonization without further purification.

Methods

Sample preparation

The selected biomass materials were first carbonized at low temperatures (150 to 180 °C) under ambient pressure (0.1 MPa) in an acidic IL {[SBMIM][HSO_4]}, followed by activation at 500 °C for 2 h in a CO_2 atmosphere. In a typical preparation process, 20 g of [SBMIM][HSO_4] was placed in a flask in an oil bath at 150 °C. Subsequently, 2 g of the biomass material was added to the [SBMIM][HSO_4] solution with magnetic stirring for 5 h for ionothermal carbonization. To achieve special morphologic bio-chars, SDS, EG, and SO surfactants were mixed with [SBMIM][HSO_4] at a weight ratio of 1/20 for the ionothermal carbonization. The resultant bio-chars were washed separately several times with ethanol and distilled water to remove residual [SBMIM][HSO_4] and the surfactants. They were dried by a freezing dryer (FDU-1200, Tokyo Rikakikai Co., Ltd.) in a high vacuum at -48 °C for 72 h, followed by heating in an oven (WFO-710, Tokyo Rikakikai Co., Ltd) at 105 °C for 3 h; afterwards, they underwent physico-chemical property analysis. The obtained bio-chars were further activated under a CO_2 atmosphere in a tubular furnace (SGL-1100, Daheng Optical Precision Machinery Co., Ltd., Shanghai) that was heated to 500 °C (at a heating rate of 10 °C/min) for 2 h to yield activated bio-chars.

Characterization methods

Elemental compositions of samples were determined by an organic elemental analyzer using an Analysensysteme GmbH D-63452 apparatus (Elementar; Hanau, Germany). BET surface area was measured using an automated surface area & pore size analyzer (Autosorb-1-MP, Quanta chrome Instruments; Boynton Beach, Florida) interfaced to a computer. The sample was treated at 300 °C for 5 h before measurement. The thermo-gravimetric analysis (TGA) was carried out in STA 409 PC/PG TG-DTA (Netzsch, Selbe, Germany) with a nitrogen flow of 60 cm^3/min at a heating rate of 10 °C/min up to 800 °C. Fourier transform infrared (FT-IR) spectroscopy (Bruker Tensor 27, Saarbrucken, Germany) was used to characterize the changes of the chemical structure of bio-chars. Samples were prepared by mixing 1.5~2.0 mg of bio-char powder sample with 400 mg KBr (Merck, for spectroscopy). The scanning range was set from 400 to 4000 cm^{-1}. Raman microspectroscopy was conducted using a continuous laser source at 514.5 nm coupled with an inVia Raman microscope (Renishaw Inc., Gloucestershire, UK). The bio-char sample was distributed evenly in water-ethanol mixtures (1:1 volume ratio) and deposited on smooth silver substrates, and then dried at 105 ^oC before testing. Structural examination of the samples was observed in an FEI Quanta 200 scanning electron microscope (SEM; Philips, PSV Eindhoven, Netherlands) at an accelerating voltage of 20 kV. In the preparation of sample, 20 mg of the bio-char was deposited evenly on an aluminium stud covered with conductive adhesive carbon tapes, and then coated with Au for 10 min to prevent charging during observations. The transmission electron microscopic (TEM) observations were conducted by a JEM-2000 EX (JEOL Ltd., Tokyo) electron microscope operating at an accelerating voltage of 200 kV. Preparation of sample for TEM is as follows: Bio-char sample was placed in a tube filled with ethanol and treated with ultrasonic for 15 min. Large particles were

precipitated from ehtanol after 3 min sedimentation. Suspension was soaked up and then dripped onto a copper support network.

RESULTS AND DISCUSSION

In a previous study (Guo *et al.* 2012b), glucose dehydration in an IL [BMIM][Cl] (1-butyl-3-methylimidazoliumchloride) catalyzed by lignin-derived carbonaceous catalyst was found to improve dehydration efficiency by the hydrogen-bonding interactions between [BMIM][Cl] and glucose. In this study, [SBMIM][HSO_4] was used as both acid catalyst and solvent for the ionothermal carbonization of biomass. The activity of [SBMIM][HSO_4] was similar to sulphuric acid, attributed mostly to its high density of acidic centers on both the cation and anion. The mechanism of bio-char formation in [SBMIM][HSO_4] was similar to that of hydrothermal carbonization (Lee *et al.* 2010a): inter molecular dehydration, aldol condensation, and aromatic group (*i.e.*, C=O, C=C, C–O–C and C–O–H) formation.

Table 1. Preparation Conditions, Elemental Compositions, and Product Yields for Bio-chars Obtained from the Carbonization of Biomasses in [SBMIM][HSO_4] at 150 to 180 °C

Test #	Bio-char code*	Preparation condition		Elemental compositions (wt%)					O/C molar ratio	Bio-char yield (wt.%)
		Temp. (°C)	Time (h)	C	H	O	S	N		
	GL	-	-	40.00	6.67	53.33	-	-	1.00	-
Test 1	GL-150(1)	150	1	61.49	4.64	31.84	2.35	1.35	0.39	40.05
Test 2	GL-150(2)	150	2	60.48	4.37	33.09	1.65	0.38	0.41	41.90
Test 3	GL-150(3)	150	3	61.95	4.38	31.98	1.27	0.30	0.39	38.75
Test 4	GL-150(4)	150	4	60.48	4.29	31.52	1.18	0.34	0.39	38.25
Test 5	GL-150(5)	150	5	61.33	4.33	32.31	1.57	0.38	0.40	37.80
Test 6	GL-160	160	5	60.03	4.22	33.22	1.64	0.29	0.42	37.50
Test 7	GL-170	170	5	60.23	4.20	33.53	2.29	0.39	0.42	36.55
Test 8	GL-180	180	5	59.78	4.07	33.85	2.25	0.36	0.42	37.40
Test 9	GL-SDS-150	150	5	63.76	4.38	30.36	0.61	0.51	0.36	33.77
Test 10	GL-EG-150	150	5	65.56	5.27	29.84	1.24	0.47	0.34	25.57
Test 11	GL-SO-150	150	5	69.56	6.68	23.54	0.45	0.18	0.25	62.55
	CE	-	-	43.29	6.17	51.62	0.34	0.14	0.89	-
Test 12	CE-150	150	5	61.66	4.78	33.25	1.85	0.77	0.40	50.40
	LI	-	-	52.24	4.51	33.50	4.74	0.20	0.48	-
Test 13	LI-150	150	5	55.33	5.12	30.70	6.10	2.45	0.42	28.80
	BA	-	-	48.09	5.70	44.97	0.20	0.36	0.70	-
Test 14	BA-150	150	5	61.43	4.72	31.69	1.20	0.53	0.39	52.40

*GL, glucose; CE, cellulose; LI, lignin; BA, bamboo; SDS, sodium dodecyl sulfonate; EG, ethylene glycol; SO, sodium oleate; 150-150 °C; 150-150 °C; 160-160 °C; 170-170 °C; 180-180 °C; Other reaction conditions of carbonization: [SBMIM][HSO_4] 20 g, biomass 2 g, surfactants (SDS, EG, or SO) 1g.

The experimental results of biomass ionothermal carbonization in [SBMIM][HSO_4] are summarized in Table 1 (tests 1 through 14). Tests 1 through 8 are experiments for glucose carbonization at 150 to 180 °C. Tests 9 through 11 are

surfactant-modified glucoses carbonized at 150 °C for 5 h. Tests 12 through 14 are experiments for the carbonization of different biomass materials (cellulose, lignin, and bamboo). Abbreviated names of resulting bio-chars are also given in column 2 (Table 1). When glucose was used as a starting material (tests 1 through 11), the highest bio-char yield of 41.9% was obtained at 150 °C for 2 h and decreased to 37.8% as the reaction time increased to 5 h. However, the bio-char obtained from 2 h of carbonization displayed poor stability during the CO_2 activation. Therefore, the ionothermal carbonization conditions were chosen as 150 °C and 5 h for the subsequent experiments. Elemental analysis revealed that the carbon content increased from 40% in glucose to a range of 60 to 62% in bio-char samples (Table 1; tests 1 through 5). Increasing the reaction temperature to 180 °C from 150 °C (tests 5 through 8) led to a slight decrease of the bio-char yield, from 37.8% to 37.4%; the carbon contents and O/C molar ratio remained at approximately 60 to 61% and 0.40 to 0.42, respectively. These results suggest that temperatures at 150 to 180 °C have little influence on the elemental compositions of the bio-chars. In the ionothermal carbonization of glucose in [SBMIM][HSO_4] at 150 °C for 5 h, the addition of surfactants (*i.e.*, SDS, EG, and SO; tests 9 through 11) were beneficial for the carbon content (increased by 2.43 to 8.23%) and adverse for the O/C ratio (reduced by 0.04 to 0.15). A minimum bio-char yield of 25.57% is achieved in the EG modified ionothermal carbonization of glucose. This may be partially due to the reaction between glucose and glycol to form glycol glucoside in the presence of acidic catalyst {[SBMIM][HSO_4]} (Yamada and Ono 2001). The glucose consumption results in a decrease in the yield of the bio-char product. The maximum bio-char yield of 62.55% was found in SO-templated ionothermal carbonization. It was presumed that oleic acid, an unsaturated fatty acid, could be formed from OS in an acidic environment and underwent polymerization at high temperatures such as 150 ^oC (Goebel 1947). The resultant polymers have high viscosity and coated on the surface of bio-chars, as shown in the SEM image of GL-SO-150 (Fig. 5d). After carbonization at 150 °C and 5 h (Table 1; tests 12 through 14), the carbon contents of cellulose, lignin, and bamboo increased from 43.29%, 52.24%, and 48.09% to 61.66%, 55.33%, and 61.43%, respectively. The carbon content of lignin changed little (only 3.09%). A general view point is that lignin has the highest stability due to its aromatic structure, with the highest heating value compared with that of glucose and cellulose (Guo *et al.* 2012b). Moreover, relatively weak bonds (alkyl-arylether bond) were broken and more resistant condensed structures were formed under mild reaction conditions (Demirbaş 2000). A low bio-char yield of 28.8% from lignin was attributed to the ethanol-soluble phenolic extractives released from the degradation product of lignin during the purification step (Li *et al.* 2012). The obtained bio-chars have very low BET surface area (< 10 m^2/g). To increase the BET surface area, activation with carbon dioxide at higher temperatures was needed.

Bio-chars were further activated by carbon dioxide at 500 °C for 2 h. The BET surface area, pore diameter, and pore volume of resultant activated bio-chars are listed in Table 2. Activation experiments 1 through 4 for the glucose bio-chars (from tests 5 through 8), activations 5 through 7 for the different biomass bio-chars (CE-150, LI-150, and BA-150 from tests 12 through 14), and activations 8 through 10 for the surfactant-modified glucose bio-chars (GL-SDS-150, GL-EG-150, and GL-SO-150 from tests 9 through 11) were conducted.

Table 2. Elemental Compositions and Pore Properties of the Activated Bio-char at 500 °C

No.	Activated bio-char code*	Elemental compositions (wt%)					O/C molar ratio	Activated bio-char yield (wt.%)	Surface area (m^2/g)	Pore diameter (nm)	Pore volume (cm^3/g)
		C	H	O	S	N					
1	GL-150(5)-AC	85.24	3.08	10.00	0.10	0.28	0.088	54.70	453.94	3.55	0.098
2	GL-160-AC	85.29	3.13	10.72	0.053	0.27	0.094	54.73	452.89	3.55	0.072
3	GL-170-AC	83.92	3.28	11.65	0.14	0.33	0.104	55.40	469.79	3.59	0.104
4	GL-180-AC	85.49	3.13	11.65	0.054	0.31	0.102	57.46	448.43	3.62	0.070
5	CE-AC	84.88	3.65	11.19	0.17	0.58	0.099	58.30	465.48	3.58	0.164
6	LI-AC	84.45	2.95	10.19	0.14	0.58	0.090	50.38	289.18	3.58	0.037
7	BP-AC	85.73	3.32	9.92	0.13	0.58	0.087	60.82	430.72	3.57	0.066
8	GL-SDS-AC	84.46	3.43	10.99	0.14	0.73	0.098	58.76	432.03	3.58	0.059
9	GL-EG-AC	86.29	3.48	11.27	0.12	0.31	0.098	51.21	391.44	3.62	0.043
10	GL-SO-AC	86.40	3.57	11.17	0.14	0.61	0.097	55.97	448.43	3.61	0.112

* The activated bio-chars obtained from GL-150, GL-160, GL-170, GL-180, CE-150, LI-150, BP-150, GL-SDS-150, GL-EG-150, and GL-SO-150 are defined as GL-150-AC, GL-160-AC, GL-170-AC, GL-180-AC, CE-AC, LI-AC, BP-AC, GL-SDS-AC, GL-EG-AC, and GL-SO-AC, respectively (AC-activated carbon).

The elemental compositions (*i.e.*, C, H, N, and O contents) of all activated bio-chars were slightly different. The pore diameter range from 3.55 to 3.62 nm suggests that mesoporous skeleton carbons were formed after CO_2 activation. The activated bio-char yield, BET surface area, and pore volume were influenced by raw materials and surfactants (Table 2). The BET surface area of activated bio-chars ranged from 430.7 to 469.8 m^2/g, except for activation 6 (LI-AC, 289.2 m^2/g) and activation 9 (GL-EG-AC, 391.4 m^2/g). The lower BET area of GL-EG-AC was possibly due to the formation of membrane structure (Fig. 5c). The pore volume of activated glucose bio-chars (activations 1 through 4) increased from 0.098 to 0.104 cm^3/g as the carbonization temperature at first step increased from 150 to 170 °C, but fell to 0.070 cm^3/g as the temperature further increased to 180°C. It has been reported that initial porosity is created during carbonization, but further developed in the activation process (Li *et al.* 2008). Moreover, the addition of a non-ionic surfactant (EG, activation 9) decreased BET surface area and pore volume of the activated bio-char by 62 m^2/g and 0.055 cm^3/g, respectively, compared with that of GL-150(5)-AC (activation 1). In contrast, anionic surfactants (SDS and SO) had little influence on surface area and pore volume, although a previous study has reported an influence (Li *et al.* 2008). By using different surfactants, it is possible to tailor activate bio-chars for specific structures.

The chemical transformations induced by ionothermal carbonization in [SBMIM][HSO_4] are examined by Raman microspectroscopy and FT-IR. Figure 1 shows Raman spectra of glucose-derived bio-chars obtained by the ionothermal carbonization step [test 5, GL-150(5)] and subsequent CO_2 activation [activation 1, GL-150(5)-AC].

The bio-chars obtained by ionothermal carbonization showed no G-band or D-band (Fig. 1a). After CO_2 activation, the activated bio-char exhibits two broad overlapping bands around 1355 and 1590 cm^{-1} (Fig. 1b). These bands correspond to the D- and G-modes of sp^2 atoms in condensed benzene rings of amorphous carbon, respectively (Sevilla and Fuertes 2009). Therefore, a graphitic structure was formed in activated bio-chars (Guo *et al.* 2012b).

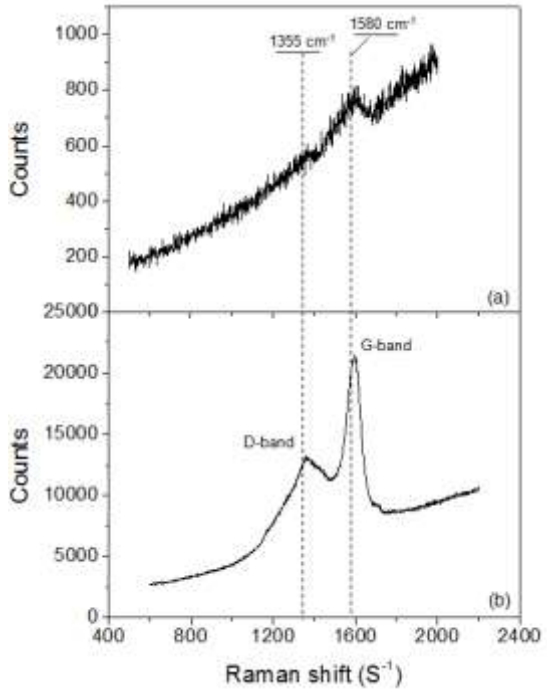

Fig.1. Raman spectra of bio-chars obtained from glucose: (a) carbonization [test 5, GL-150(5)], and (b) subsequent CO_2 activation [activation 1, GL-150(5)-AC]

FT-IR spectra of glucose-derived bio-chars obtained at different ionothermal carbonization temperatures (tests 5 through 8) are illustrated in Fig. 2a. The corresponding FT-IR spectrum band assignments are summarized in Table 3 (Bio-Rad Laboratories 2004; Lee *et al.* 2010; Sevilla and Fuertes 2009; Tanaka*et al.* 2005). All four bio-chars show strong broad absorption bands at 3433 cm^{-1}, which are attributed to OH stretching vibration in hydroxyl groups. The band at 1710 cm^{-1} is due to C=O vibrations in carbonyl, quinone, ester, or carboxyl (Sevilla and Fuertes 2009; Tanaka *et al.* 2005). The C=C stretching vibrations in aromatic rings are visible in the spectra at 1625 cm^{-1} (Sevilla and Fuertes 2009). The bands at 1210 and 1037 cm^{-1} may be connected with cyclic C–O–C and C–O–H groups, respectively (Lee *et al.* 2010; Tanaka *et al.* 2005). The band observed at 802 cm^{-1} is assigned to aromatic hydrogen (Bio-Rad Laboratories 2004; Lee *et al.* 2010). These results demonstrate that the aromatization occurred during carbonization, which was consistent with the results from the Raman spectra. The FT-IR spectra of the bio-chars derived from ionothermal carbonization were similar to those of sulfurated carbonaceous catalysts in a previous study. Both types of chars have absorption peaks at ~810, ~1610 and ~1720 cm^{-1} (Guo *et al.* 2012c). These results suggested that the acidic IL {[SBMIM][HSO_4]} has similar catalytic behavior action to sulphuric acid during the carbonization. However, this reaction was weakly influenced by carbonization temperatures because the absorption band of aromatic C–H changed slightly.

Table 3. Fourier Transform Infrared (FT-IR) Spectrum Band Assignments

Main observed bands (cm^{-1})	Assignments
802	Aromatic C-H out of plane bending vibrations
1034, 1059	C-OH stretching vibration in -CHOH group
1181	C-OH stretching vibration in phenols
1112, 1131, 1165, 1210	C-O-C (hydroxyl, ester, or aromatic ether) stretching vibrations
1340	C-N stretching vibration in aromatic ring
1372	O-H bending vibrations in phenols
1432	O-H in-plane deformation
1510	NO_2 asymmetric stretching
1533	C=O stretching and C=C stretching
1498, 1618, 1598, 1609, 1624, 1632	C=C stretching vibrations in olefinic double bonds
1709,1715	C=O (carbonyl, quinone, ester, or carboxyl)
2853, 2924	Aliphatic C-H stretching vibrations
3420～3440	O-H stretching vibrations (hydroxyl or carboxyl)

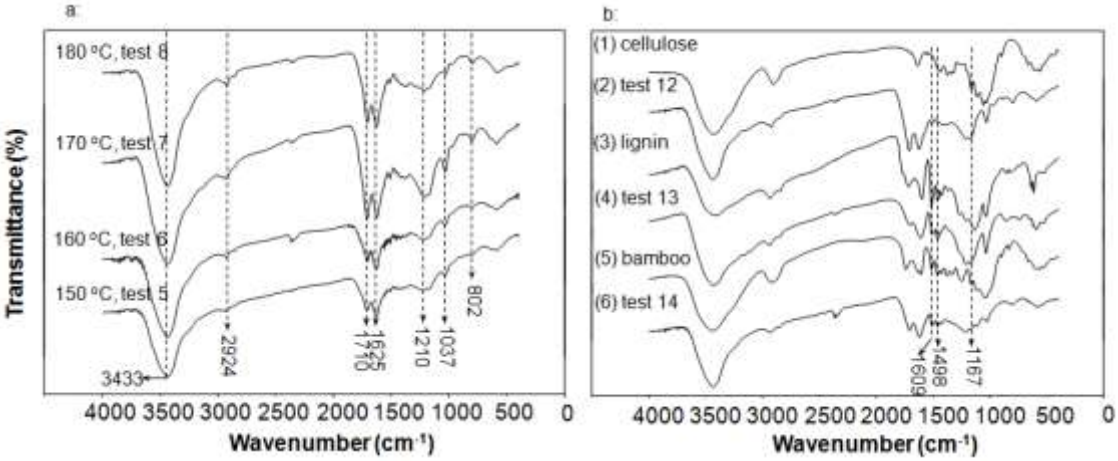

Fig. 2. Fourier transform infrared (FT-IR) spectra of: (a) bio-chars from glucose obtained at different carbonization temperature (tests 5-8); (b) different biomasses and their bio-chars: (1) cellulose; (2) CE-150 (test 12); (3) lignin; (4) LI-150 (test 13); (5) bamboo; (6) BA-150 (test 14)

Figure 2b gives FT-IR spectra of different biomasses and their derived bio-chars (tests 12 through 14). Five typical groups (C=O, C=C, C–O–C, C–O–H, and C–H) were also found in these bio-chars from cellulose, lignin, and bamboo. Compared with the spectrum of cellulose (Fig. 2b-1), two new vibration bands at 1710 and 802 cm^{-1}, corresponding to C=O and aromatic C–H (Bio-Rad Laboratories 2004; Lee *et al.* 2010; Tanaka *et al.* 2005), respectively, appear in the spectrum for bio-char CE-150 (test 12, Fig. 2b-2). Similarly, there is a significant difference between the spectra of lignin (Fig. 2b-3) and its bio-char LI-150 (test 13, Fig. 2b-4), and the appearance of new vibration bands at 1167 (C–O–C stretching), 1498 (C=C stretching), and 1609 cm^{-1} (C=C stretching) (Bio-Rad Laboratories 2004; Lee *et al.* 2010; Tanaka *et al.* 2005), while the absorption band at 800 cm^{-1} was not found. It can be concluded that intra-molecular and inter-molecular dehydration occurred during the carbonization in IL. It is interesting to note that there is a strong resemblance between the spectrum of BA-150 (test 14, Fig. 2b-6) and those of GL-150 (test 5, Fig. 2a) and CE-150 (test 12, Fig. 2b-2), except for two new bands at 1500 and 1460 cm^{-1}, assigned to C=C and C–O–H groups, respectively

(Bio-Rad Laboratories 2004; Sevilla and Fuertes 2009). The FT-IR spectrum of LI-150 is distinctly dissimilar to those of GL-150 and CE-150, due to its specific structure and elementary composition. As previously mentioned, lignin remained stable during carbonization in IL and subsequent CO_2 activation, and partial typical groups (*i.e.*, C–O–C in aromatic ether at 1128 cm^{-1}, heteroaryl C=C at 1498, and 1609 cm^{-1}) were preserved. The thermal stability of bio-chars from the ionothermal carbonization step was markedly improved by CO_2 activation at the high temperature of 500 °C, except in bamboo-derived bio-chars (Fig. 3). The increase of both carbon content (Tables 1 and 2) and degree of aromatic condensation leads to an increase in the thermal stability.

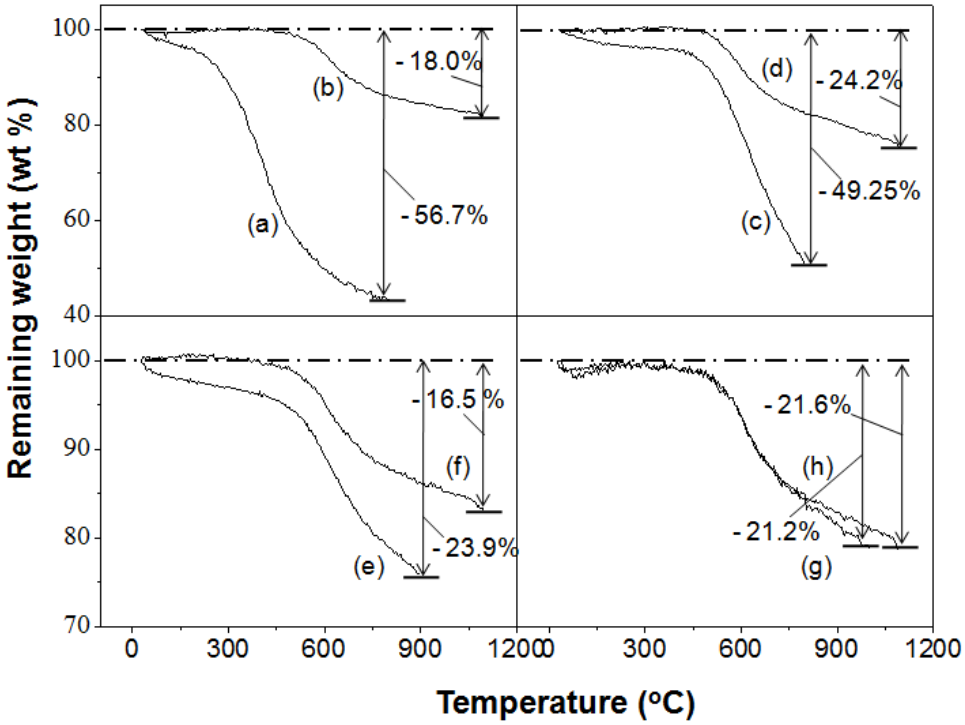

Fig. 3. Thermo-gravimetric (TG) curves of bio-chars: without activation: (a) GL-150, (c) CE-150, (e) LI-150, (g) BA-150; with activation: (b) GL-150-AC, (d) CE-AC, (f) LI-AC, (h) BA-AC

Furthermore, the effect of surfactants on glucose bio-chars can also be analyzed using the FT-IR spectra (Fig. 4). Compared with the spectrum of GL-150 (Fig. 4a-1), absorption bands of C=O (1709 cm^{-1}), C–O–C (1209 cm^{-1}), and C–OH (1036 cm^{-1}) in surfactant-templated bio-chars (GL-SDS-150 and GL-EG-150) were evidently strengthened (Fig. 4a-2 and 4a-3). These results suggest that the surfactant-modified ionothermal carbonization is conducive to achieving more functional groups. However, GL-SO-150 (Fig. 4a-4) shows a weak absorption band at 1625 cm^{-1} (C=C), indicating SO has a negative effect on glucose carbonization. After CO_2 activation at 500 °C, the FT-IR spectra of all bio-chars displayed similar changes (Figs. 4b-5 through 4b-8). The absorption strength of bands at 1709 (C=O), 1209 (C–O–C), and 1034 cm^{-1} (C–OH) weakens greatly due to oxygen removal. The results are concordant with that of elemental composition (Table 2). The weakness of C=O and C-O-H band suggest that aldol condensation occurred between aldehyde group and hydroxyl group. The enhancement of C=C band confirmed the intermolecular dehydration reaction. All these reactions led to

the loss of oxygenated functional groups at samples surface. On the other hand, strengthening of C=C groups at 1625 cm^{-1} and a new absorption band of aromatic C–H at 854 cm^{-1} (Figs. 4b-5 through 4b-8) compared with that of GL-150 (Fig. 4a-1) indicated that aromatization of activated bio-chars by condensation and dehydration further occurred at a high temperature of 500 °C. Although the functional groups on the surface of carbons are produced by CO_2activation (Molina-Sabio*et al.* 1996), in this study CO_2 activation led to the reduction of oxygen containing functional groups at relatively high temperatures (Tables 1 and 2).

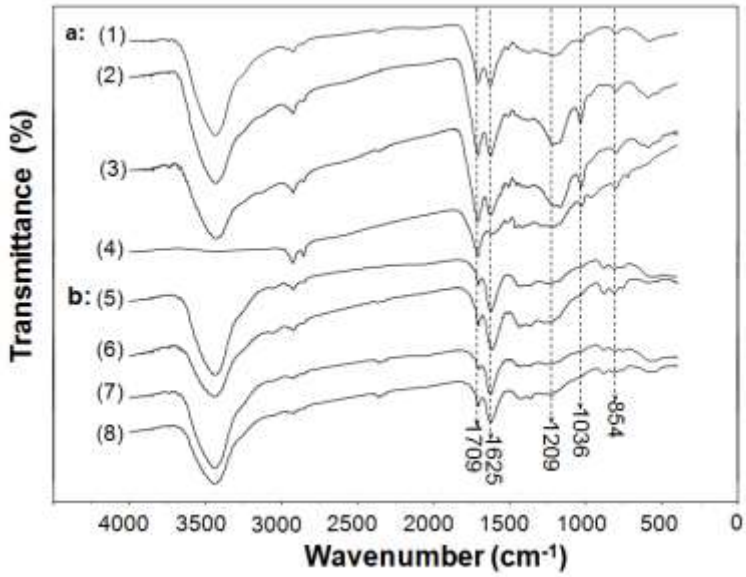

Fig. 4. FT-IR spectra of bio-chars from glucose without/with surfactant-template: (a) without activation: (1) GL-150, (2) GL-SDS-150, (3) GL-EG-150, (4) GL-SO-150; (b) with activation: (5) GL-AC; (6) GL-SDS-AC; (7) GL-EG-AC; (8) GL-SO-AC

The micro structure reformation of resultant bio-chars was more significant when surfactants were used as templates. The SEM micrographs of surfactant-templated bio-chars illustrate the great structural differences between the surfactant-templated bio-chars from the ionothermal carbonization (Figs. 5b through 5d) and CO_2 activation (Figs. 5f through 5h). Bio-chars from the ionothermal carbonization step, such as GL-150, GL-SDS-150, and GL-SO-150, consisted of an amorphous and heterogeneous spherical structure about 0.5 to 1.5 μm in diameter. The smooth surface observed for GL-SO-150 may be partially due to the fusion process of the intermediates from the carbonization reaction and SO. It is interesting to note that a carbon membrane about 70 nm in thickness was formed by adding EG in [SBMIM][HSO_4] (Fig. 5c), which is difficult to form by traditional hydrothermal carbonization (Lee *et al.* 2010a). It has been suggested that polyols can serve as reducing agents to control particle growth and prevent inter-particle aggregation (Cai and Wan 2007). The use of both surfactants and CO_2 activation altered the surface morphology of resultant bio-chars. Increased porosity (3.55 to 3.62 nm pore diameter; Table 2) and decreased diameter (about 200 nm) from volatiles escaping during CO_2 activation were also observed (Figs. 5e and 5h). It is exciting to note that the carbon membrane structure was perfectly preserved after CO_2 activation, as well as the morphology of GL-150 and GL-SO-150 (Fig. 5g). The SEM images show the morphology of GL-SDS-AC (Fig. 5f) with special rod-like structures (~200 nm

diameter). Moreover, a few fragmentary and dispersive microspheres were formed around a rod-like carbon. It can be speculated that GL-150, GL-EG-150 and GL-SO-150 were more stable than GL-SDS-150, after activation, they can find applications in catalyst supports due to their abundant surface functional groups and high surface areas.

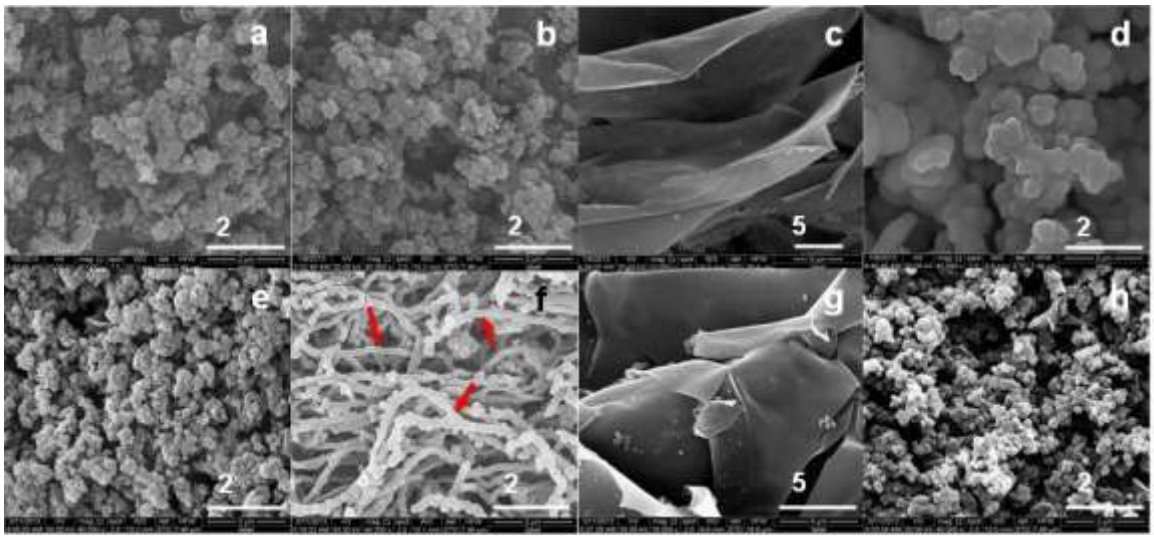

Fig. 5. Scanning electron microscope (SEM) images of bio-chars from glucose without/with surfactant-template without activation: (a) GL-150, (b) GL-SDS-150, (c) GL-EG-150, (d) GL-SO-150; and with activation: (e) GL-AC, (f) GL-SDS-AC, (g) GL-EG-AC, (h) GL-SO-AC

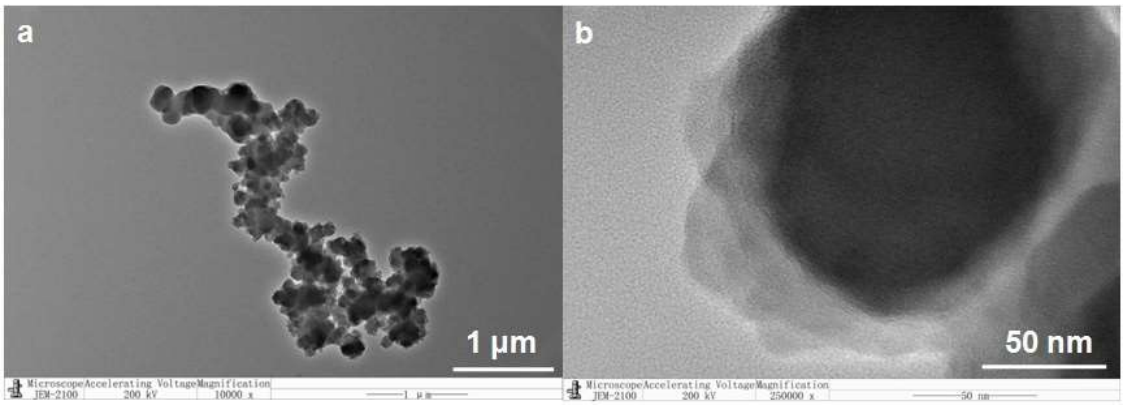

Fig. 6. Transmission electron microscope (TEM) images of the activated bio-char from surfactant-templated glucose (GL-SDS-AC): (a) low magnification (10000X) and (b) high magnification (250000X)

The TEM image of GL-SDS-AC indicates a stacking of the irregular spherical particles oriented non-directionally (Fig. 6a), and the irregular spherical particles are composed of nano-membranes in a loose accumulation (Fig. 6b). This specific spherical structure may result from different chemical compositions between the hydrophobic core and the hydrophilic shell of spherical particles (Lee *et al.* 2010). Rod-like mesoporous carbon materials are normally achieved by a traditional two-step process (Che *et al.* 2003) in which the mold with mesoporous silica materials is used as a template with subsequent dissolution of the silica framework in an acid solution. Unlike the traditional method, a novel two-step method of surfactant-templated carbonization in acidic IL and subsequent

CO_2 activation was established in this study to efficiently synthesize rod-like and other advanced morphological bio-chars. Specifically, the carbon membrane may have potential for applications such as membranes, chemical sensors, reactors membranes, and membrane catalytic electrodes (Lee *et al.* 2010a).

CONCLUSIONS

1. A two-step method, ionothermal carbonization in acidic IL followed by CO_2 activation, was employed to synthesize activated bio-chars from biomass. The IL 1-sulfobutyl-3-methylimidazolium hydrogen sulfate was demonstrated to be both an excellent acid catalyst and solvent for the ionothermal carbonization process due to its high acid density, non-volatility, and thermal stability.
2. The effect of ionothermal carbonization temperature, at the first step, on the thermal characteristics of bio-chars was negligible. The highest bio-char yield of 41.9% was obtained at 150 °C and 2 h. Biomass such as glucose, cellulose, lignin, and bamboo displayed different carbonization natures. FT-IR spectra demonstrated that the mechanism of ionothermal carbonization in acidic IL was similar to that of hydrothermal carbonization.
3. After CO_2 activation, the BET surface area and pore diameter of activated bio-chars were 289 to 469 m^2/g and 3.546 to 3.617 nm, respectively. By combination of surfactant-templated ionothermal carbonization and CO_2 activation, three different well-controlled morphologies [nano-membrane (70 nm in thickness), rod-like (200 nm in diameter), and spherical (~200 nm) mesoporous] were easily prepared under ambient pressure.
4. The method established in this work opens up a novel process for the shape-controlled synthesis of functionally activated bio-chars from low-cost biomass. However, further study needs to be performed to improve the surface area and porosity of these materials.

ACKNOWLEDGMENTS

The financial support for this research by the Chinese Academy of Sciences [the West Light Foundation and the CAS 135 program (XTBG-T02)], Natural Science Foundation of Yunnan Province of China (2011FB111), and National Natural Science Foundation of China (No:31270620) is gratefully acknowledged.

REFERENCES CITED

Bio-Rad Laboratories (2004). *The Sadtler Handbook of Infrared Spectra*, Philadelphia.

Cai, W., and Wan, J. (2007). "Facile synthesis of superparamagnetic magnetite nanoparticles in liquid polyols," *J. Colloid Interf. Sci.* 305(2), 366-370.

Carrott, P. J. M., and Ribeiro Carrott, M. M. L. (2007). "Lignin -From natural adsorbent to activated carbon: A review," *Bioresource Technol.* 98(12), 2301-2312.

Che, S., Garcia-Bennett, A. E., Liu, X., Hodgkins, R. P., Wright, P. A., and Zhao, D. (2003). "Synthesis of large-pore Ia3d mesoporous silica and its tubelike carbon replica," *Angew. Chem*. 115(33), 4060-4064.

Choma, J., Dziura, A., Gorka, J., and Jaroniec, M. (2011). "Adsorption properties of micro-/meso-porous carbons obtained by colloidal templating and post-synthesis KOH activation," *Adsorpt. Sci. Technol*. 29(5), 457-465.

Danish, M., Hashim, R., Ibrahim, M.N.M., and Sulaiman, O. (2013). "Characterization of physically activated acacia mangiumwood-based carbon for the removal of methyl orange dye," *BioResources* 8(3), 4323-4339.

Demir-Cakan, R., Makowski, P., Antonietti, M., Goettmann, F., and Titirici, M. M. (2010). "Hydrothermal synthesis of imidazole functionalized carbon spheres and their application in catalysis," *Catal. Today* 150(1-2), 115-118.

Demirbaş, A. (2000). "Effect of lignin content on aqueous liquefaction products of biomass," *Energ.Convers. Manage*. 41(15), 1601-1607.

Deng, Y., Wei, J., Sun, Z., and Zhao, D. (2013). "Large-pore ordered mesoporous materials templated from non-pluronicamphiphilic block copolymers," *Chem. Soc. Rev*. 42(9), 4054-4070.

Earle, M. J., and Seddon, K. R. (2000). "Ionic liquids. Green solvents for the future," *Pure Appl. Chem*. 72(7), 1391-1398.

Gao, J. J., Kong, D. D., Wang, Y. F., Wu, J., Sun, S. L., and Xu, P. (2013). "Production of mesoporous activated carbon from tea fruit peel residues and its evaluation of methylene blue removal from aqueous solutions," *BioResources* 8(2), 2145-2160.

Goebel, C.G. (1947). "Polymerization of unsaturated fatty acids," *J. Am. Oil Chem.* 24(3), 65-68.

Guo, F., Fang, Z., Xu, C. C., and Smith Jr., R. L. (2012a). "Solid acid mediated hydrolysis of biomass for producing biofuels," *Prog. Energ. Combust*. 38(5), 672-690.

Guo, F., Fang, Z., and Zhou, T. J. (2012b). "Conversion of fructose and glucose into 5-hydroxymethylfurfural with lignin-derived carbonaceous catalyst under microwave irradiation in dimethyl sulfoxide-ionic liquid mixtures," *Bioresource Technol*. 112, 313-318.

Guo, F., Xiu, Z. L. and Liang, Z. X. (2012c). "Synthesis of biodiesel from acidified soybean soapstock using a lignin-derived carbonaceous catalyst," *Appl. Energy* 98, 47-52.

Hameed, B. H., Din, A. T. M., and Ahmad, A. L. (2007). "Adsorption of methylene blue onto bamboo-based activated carbon: Kinetics and equilibrium studies," *J. Hazard. Mater.* 141(3), 819-825.

Hu, Z. H., and Srinivasan, M. P. (1999). "Preparation of high-surface-area activated carbons from coconut shell," *Micropor. Mesopor. Mat*. 27(1), 11-18.

Hu, Z. H., and Srinivasan, M. P. (2001). "Mesoporous high-surface-area activated carbon," *Micropor. Mesopor. Mat*. 43(3), 267-275.

Ioannidou, O., and Zabaniotou, A. (2007). "Agricultural residues as precursors for activated carbon production-A review," *Renew. Sust. Energ. Rev*. 11(9), 1966-2005.

Kruk, M., Jaroniec, M., and Bereznitski, Y. (1996). "Adsorption study of porous structure development in carbon blacks," *J. Colloid. Interface Sci*. 182(1), 282-288.

Lee, J. S., Mayes, R. T., Luo, H., and Dai, S. (2010a). "Ionothermal carbonization of sugars in a protic ionic liquid under ambient conditions," *Carbon* 48(12), 3364-3368.

Lee, J. S., Wang, X., Luo, H., and Dai, S. (2010b). "Fluidic carbon precursors for formation of functional carbon under ambient pressure based on ionic liquids," *Adv. Mater*. 22(9), 1004-1007.

Lee, J. S., Wang, X., Luo, H., Baker, G. A., and Dai, S. (2009). "Facile ionothermal synthesis of microporous and mesoporous carbons from task specific ionic liquids," *J. Am. Chem. Soc*. 131(13), 4596-4597.

Li, M. F., Sun, S. N., Xu, F., and Sun, R. C. (2012). "Ultrasound-enhanced extraction of lignin from bamboo (*Neosinocalamus affinis*): Characterization of the ethanol-soluble fractions," *Ultrason. Sonochem*. 19(2), 243-249.

Li, W., Yang, K., Peng, J., Zhang, L., Guo, S., and Xia, H. (2008). "Effects of carbonization temperatures on characteristics of porosity in coconut shell chars and activated carbons derived from carbonized coconut shell chars," *Indust. Crops Prod*. 28(2), 190-198.

Liu, X. J., Guo, M. L., Huang, J., and Yin, X. Y. (2013). "Improved fluorescence of carbon dots prepared from biogases under alkaline hydrothermal conditions," *BioResources* 8(2), 2537-2546.

Mizuta, K., Matsumoto, T., Hatate, Y., Nishihara, K., and Nakanishi, T. (2004). "Removal of nitrate-nitrogen from drinking water using bamboo powder charcoal," *Bioresource Technol*. 95(3), 255-257.

Molina-Sabio, M., Gonzalez, M.T., Rodriguez-Reinoso, F., and Sepúlveda-Escribano, A. (1996). "Effect of steam and carbon dioxide activation in the micropore size distribution of activated carbon," *Carbon* 34(4), 505-509.

Paraknowitsch, J. P., and Thomas, A. (2012). "Functional carbon materials from ionic liquid precursors," *Macromol. Chem. Phys*. 213(10-11), 1132-1145.

Sekar, M., Sakthi, V., and Rengaraj, S. (2004). "Kinetics and equilibrium adsorption study of lead (II) onto activated carbon prepared from coconut shell," *J. Colloid. Interf. Sci.* 279(2), 307-313.

Sevilla, M., and Fuertes, A. B. (2006). "Chemical and structural properties of carbonaceous products obtained by hydrothermal carbonization of saccharides," *Chem. Eur. J*. 15(16), 4195-4203.

Sevilla, M., and Fuertes, A. B. (2009). "The production of carbon materials by hydrothermal carbonization of cellulose," *Carbon* 47(9), 2281-2289.

Simon, P., and Gogotsi, Y. (2008). "Materials for electrochemical capacitors," *Nat. Mater*. 7, 845-854.

Sircar, S., Golden, T. C., and Rao, M. B. (1996). "Activated carbon for gas separation and storage," *Carbon* 34(1), 1-12.

Stoller, M. D., Park, S., Zhu, Y., An, J., and Ruoff, R. (2008). "Graphene-based ultracapacitors," *NanoLett*. 8(10), 3498-3502.

Tanaka, S., Nishiyama, N., Egashira, Y., and Ueyama, K. (2005). "Synthesis of ordered mesoporous carbons with channel structure from an organic-organic nanocomposite," *Chem. Commun*. 16, 2125-2127.

Titirici, M. M., and Antonietti, M. (2010). "Chemistry and materials options of sustainable carbon materials made by hydrothermal carbonization," *Chem. Soc. Rev.* 39, 103-116.

Wang, X., and Dai, S. (2010). "Ionic liquids as versatile precursors for functionalized porous carbon and carbon oxide composite materials by confined carbonization," *Angew. Chem. Int. Ed*. 49(37), 6664-6668.

Wang, X., Liang, C., and Dai, S. (2008). "Facile synthesis of ordered mesoporous carbons with high thermal stability by self-assembly of resorcinol-formaldehyde and block copolymers under highly acidic conditions," *Langmuir* 24(14), 7500-7505.

Welton, T. (2004). "Ionic liquids in catalysis," *Coordin. Chem. Rev*. 248, 2459-2477.

Wu, Y. Y., Zhang, C., Liu, Y. C., Fu, Z. H., Dai, B. H., and Yin, D. L. (2012). "Biomass char sulfonic acids (BC-SO_3H)-catalyzed hydrolysis of bamboo under microwave irradiation," *BioResources* 7(4), 5950-5959.

Xie, Z. L., White, R. J., Weber, J., Taubert, A., and Titirici, M. M. (2011). "Hierarchical porous carbonaceous materials via ionothermal carbonization of carbohydrates," *J. Mater. Chem*. 21, 7434-7442.

Yamada, T., and Ono, H. (2011). "Characterization of the products resulting from ethylene glycol liquefaction of cellulose," *J. Wood Sci.* 47(6), 458-464.

Yuan, J., Giordano, C., and Antonietti, M. (2010). "Ionic liquid monomers and polymers as precursors of highly conductive, mesoporous, graphitic carbon nanostructures," *Chem. Mater*. 22(17), 5003-5012.

Article submitted: January 14, 2014; Peer review completed: March 6, 2014; Revised version received and accepted: April 10, 2014; Published: April 21, 2014.